The size of the proton

Author: Tània Tomàs Ripollés
Advisor: Mario Centelles
Facultat de Física, Universitat de Barcelona, Diagonal 645, 08028 Barcelona, Spain.*

Abstract: In this work, the atomic energy levels for hydrogen-like atoms, in particular, for muonic hydrogen are described. We discuss why this exotic atom is a good candidate to help measure the proton radius. Such experiments with muonic hydrogen have been performed very recently and have shown a "shrinkage" of the proton size in disagreement with previous measurements. This so-called "proton radius puzzle" is still under debate but we summarize some possible explanations that have been proposed.

I. INTRODUCTION

The proton is one of the most common particles in the visible Universe but some of its properties such as its charge radius are yet not precisely known. In this work we intend to review the present status of our knowledge of the root-mean-square charge radius of the proton, r_p, and the latest scientific experiments aiming to determine it. Transition frequencies in atomic hydrogen (and other exotic atoms where the electron is replaced by a heavier particle) depend on the proton size because the electric field differs from that produced by a point charge. This effect is detectable due to the accuracy with which optical frequencies can be measured. Indeed, theory of quantum electrodynamics (QED) is needed to accurately understand atomic transitions.

Until recently, the value for the proton charge radius was mainly determined using two methods: with an accuracy of 2% at best in r_p, by electron-proton scattering experiments [1,2] or using spectroscopy to measure the energy levels of electrons orbiting an atomic nucleus. The current most accurate measurement of r_p with 1% uncertainty is given by the CODATA value, based on precision spectroscopy of atomic hydrogen [3,4] and calculations of bound-state quantum electrodynamics.

The hydrogen atom is the one best studied atom to date in modern physics. In 1947 the splitting of the $2S_{1/2}$-$2P_{1/2}$ discovered by Lamb and Retherford [8] stimulated the development of the theory of QED, as Dirac's theory proved insufficient. Current tests of QED on atomic hydrogen have reached such high precision that comparison with the theory is limited by the experimental uncertainty in the proton form factors. Very recent experiments [5,6] using muonic hydrogen (where the electron is replaced by a muon) allowed for the first time to measure the 2S-2P Lamb shift of this exotic atom and have provided a different way to measure r_p, with more accuracy. As the muon is 207 times heavier than the electron, its atomic Bohr radius is also about 200 times smaller than in electronic hydrogen, thus enhancing the nuclear finite-size effects.

This new line of experiments performed in 2010 [5] and 2013 [6] on muonic hydrogen led up to a measurement of r_p =0.84184(67) fm which differs by about 5 standard deviations from the 2010 CODATA value of 0.8768(69) fm and the current CODATA value of 0.8751(61) fm, as it is shown in Fig. 1. This discrepancy is known as *The proton radius puzzle* and its origins are yet unclear.

In order to understand the reason of such discrepancy, more recent experiments with muonic deuterium [14] (where a muon orbits a nucleus of one proton and one neutron) and with electronic hydrogen [15] have been performed with new and improved techniques and calculations. The results are in agreement with the "smaller" proton size found with muonic hydrogen, furthering the proton radius puzzle.

This work has the following structure. Section II contains the corrections to atomic energy levels for hydrogen-like atoms, such as fine structure, Lamb shift and recoil corrections. In section III we introduce the muonic hydrogen and describe the experiments that measure the muonic Lamb shift aiming to determine the value of r_p. In section IV the results from new and improved experiments performed with laser spectroscopy in H are summarized. Finally, section V contains the summary and conclusions.

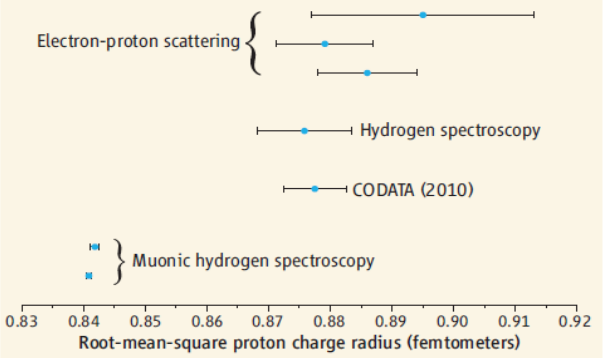

FIG. 1: Plot of the determination of r_p using different methods. The discrepancy between the 2010 CODATA value and muonic hydrogen is clear.

II. ENERGY LEVELS OF HYDROGEN-LIKE ATOMS

As the simplest of all stable atoms, hydrogen (H) allows for high-precision comparisons between theory and experiments of bound-state energy physics. The Bohr atomic model was inspired by the observation of the Balmer series in H, it introduced the quantization rules in order to explain the existence of the observed stable energy discrete levels.

Schrödinger model. In the first approximation, energy levels of hydrogen atoms are described by the solution of the Schrödinger equation of an electron in the field of an infinitely heavy Coulomb center of charge Z. They can be written as:

$$E_n(M=\infty) = -\frac{mc^2}{2n^2}(Z\alpha)^2 = -hcR_\infty \frac{Z^2}{n^2}\ , \quad (1)$$

* Electronic address: tfgac@ub.edu

where n is the principal quantum number, c is the speed of light, α is the fine structure constant, m is the electron mass and R_∞ is the Rydberg constant. Besides the principal quantum number n each state is labelled with the value for the orbital angular momentum l and its projection m. Therefore, the E_n energy levels are n times degenerate with respect to l and each level with given l is additionally $2l+1$ times degenerate.

To take into account the effect of the finite mass of the nucleus M, one has to work with the reduced mass of the two-body system $m_r = \frac{mM}{m+M}$ and the Bohr energy levels are correspondingly modified:

$$E_n = \frac{m_r}{m} E_n(M=\infty). \quad (2)$$

Dirac model. More precise measurements on H revealed a splitting of the $n=2$ states, its origins are effects arising from the spin of the electron and relativity. A proper description of all relativistic corrections to the energy levels of a spin ½ particle is given by the Dirac equation with a Coulomb source:

$$E_{nj}(M=\infty) = mc^2 f(n,j)\ , \quad (3)$$

$$f(n,j) = \left[1 + \frac{(Z\alpha)^2}{\left[n-j-\frac{1}{2}+\sqrt{\left(j+\frac{1}{2}\right)^2-(Z\alpha)^2}\right]^2}\right]^{-1/2}$$
$$\approx \left[1 - \frac{(Z\alpha)^2}{2n^2} - \frac{(Z\alpha)^4}{2n^3}\left(\frac{1}{j+\frac{1}{2}} - \frac{3}{4n}\right) + \cdots\right], \quad (4)$$

where the total angular momentum quantum number j ($\vec{J} = \vec{L} + \vec{S}$) was introduced. Now the degeneracy for the total angular momentum has been broken but energy levels are still degenerate for the orbital angular momentum l.

We must note that Dirac's energy levels do not take into account the finite mass of the proton. As the relativistic effects introduce small modifications on the energy levels (at least for small charge Z of the nucleus), it is possible to approximate the recoil correction of finite mass with the reduced mass factor:

$$E_{nj} = mc^2 + m_r c^2[f(n,j)-1]\,. \quad (5)$$

In order to provide more accurate corrections of the Dirac spectrum with the reduced mass dependence in eq. (5) they should be derived from QED and lead to the result [7]:

$$\mathrm{E_{nj}} = \mathrm{m}c^2 + \mathrm{m_r}c^2[\mathrm{f(n,j)}\text{-}1] - \frac{\mathrm{m_r^2}c^2}{2(\mathrm{m+M})}[\mathrm{f(n,j)}\text{-}1]^2 +$$
$$+ \frac{(\mathrm{Z\alpha})^4 \mathrm{m_r^3}c^2}{2\mathrm{n^3M^2}}\left(\frac{1}{\mathrm{j}+\frac{1}{2}} - \frac{1}{\mathrm{l}+\frac{1}{2}}\right)(1\text{-}\delta_{l0})\ . \quad (6)$$

We note the appearance of the last term in (6) which breaks the degeneracy in the Dirac spectrum between levels with the same j and $l = j \pm 1/2$.

Nuclear-structure corrections. Even with the Bohr radius being orders of magnitude larger than the size of the nucleus the actual theoretical and experimental level of precision is sensitive to the nuclear structure. The energy shifts from nuclear contributions involve properties of the finite nuclear volume and the nuclear magnetic moment (hyperfine splitting, HFS). The finite size contribution is non-vanishing only for S states. Since the proton charge is actually distributed over a finite volume and not point-like, the electron which is within this volume experiences a smaller attraction, leading to an energy shift given by [11]:

$$\Delta E_V = -\frac{2}{3}\frac{(Z\alpha)^4}{n^3} m_r^3 c^6 \left(\frac{r_p}{\hbar c}\right)^2, \quad (7)$$

in terms of the root-mean-square charge radius r_p of the proton, which is defined as $r_p^2 = \int r^2 \rho(\vec{r}) d\vec{r}$, where $\rho(\vec{r})$ is the proton charge distribution.

On the other hand, as the nucleus has a non-zero magnetic moment it is expected that it will interact with the electron, causing additional modifications to the energy levels, called hyperfine splitting. Treating the magnetic interaction as a perturbation, it is found that the fine-structure energy levels split depending on the angular momentum of the nucleus $\vec{I}$ and that of the nucleus and electron $\vec{F} = \vec{J} + \vec{I}$, which gives rise to additional corrections $\Delta E_{nljIF} \propto [F(F+1) - I(I+1) - j(j+1)]$.

Radiative QED corrections. Investigation on the energy levels of hydrogen revealed a small deviation from the prediction of the Dirac equation. This energy difference is known as the *Lamb shift*, its origins are quantum fluctuations and shows that energy levels depend, also, on the angular momentum l. See a schematic layout for the innermost energy levels for H in Fig. 2.

We have seen in (6) that energy levels are predicted to depend on l when introducing recoil corrections but such energy differences are too small compared to what was found experimentally, those effects arise from QED effects such as radiative corrections and vacuum polarization. The classical example of this is the energy splitting between states $2S_{1/2}$ and $2P_{1/2}$ in the hydrogen atom. It was measured for the first time by Lamb and Retherford with microwave spectroscopy [8]. Since its discovery, the Lamb shift has been well studied for hydrogen as laser spectroscopy measurements have reached extreme precision and accurate theoretical numerical predictions have been made to explain the experimental results.

Because the Lamb shift originates from quantum electrodynamics effects, S-states are more affected by this correction as the probability of the electron to be inside the nucleus is non-vanishing for l=0.

To leading order, the correction from the Lamb shift to the energy levels for hydrogen-like atoms can be expressed as [9]:

$$\Delta E_{nlj}^{LS} = \frac{4mc^2}{3\pi n^3}\alpha(Z\alpha)^4\left\{L_{nl} + \left[\frac{19}{30} - 2\ln(Z\alpha)\right]\delta_{l0} \pm \frac{3}{4}\frac{1}{(2j+1)(2l+1)}(1-\delta_{l0})\right\}, \quad (9)$$

where L_{nl} is known as the *Bethe logarithm* and has to be evaluated numerically [9]. We now see that the degeneracy with the angular momentum l has been broken and states with $l=0$ are affected differently as they have a non-zero probability to be inside the nucleus.

To achieve a still better quantitative prediction for the Lamb shift, several contributions of higher-order from QED and from the finite size of the nucleus must be included in (9).

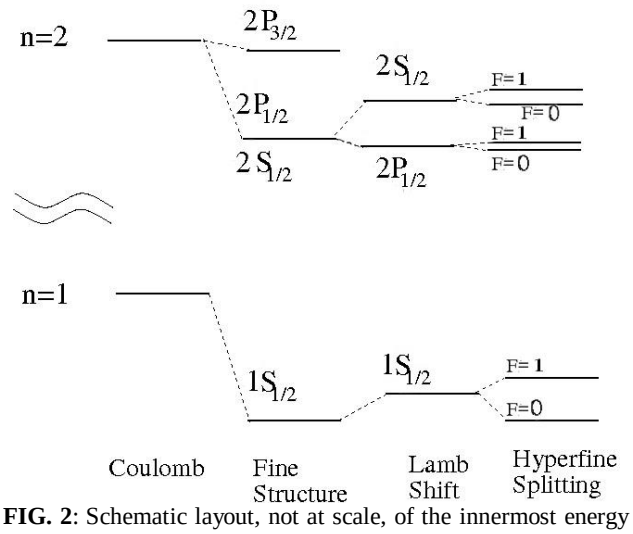

FIG. 2: Schematic layout, not at scale, of the innermost energy levels for hydrogen for the Coulomb potential, Dirac model, Lamb shift and hyperfine splitting.

These can be found in reference [7] as well as in references quoted in [13]. Today's result of theoretical value of the Lamb shift for the states $2S_{1/2}$ and $2P_{1/2}$ for hydrogen is in excellent agreement with the experiment. Yet, a source of uncertainties is the limited knowledge of the size of the proton radius. A solution for obtaining a determination of r_p with less uncertainty is using muonic hydrogen (μp); the muon's larger mass gives muonic hydrogen a smaller atomic size resulting in seven orders of magnitude larger influence of r_p on the energy levels, which allows the proton structure to be studied more accurately. A comparison between the 2S and 2P energy levels for both atoms is shown in Fig. 3 [10].

III. PROTON RADIUS FROM MUONIC HYDROGEN

A muon is an elementary particle with the same properties as the electron except its mass, being the muon 206.768 2826(46) times heavier. The muonic Bohr radius is, therefore, about 200 times smaller than for the electron; thus making finite size effects play a major role when the muon orbits a nucleus.

Production of muonic hydrogen. By inelastic scattering experiments with high-energy protons, pions are produced. They decay into muons by the weak interaction through the reaction $\pi^- \rightarrow \mu^- + \nu_\mu$. The muons are then decelerated and bombarded onto ordinary hydrogen where they are "captured", usually in one of the outer energy levels n≈14. By a cascade of radiative transitions, about 99% of the muons proceed to the 1S ground state emitting X-rays, while the remaining 1% muons populate the metastable 2S state.

Muons decay by weak interaction ($\mu^- \rightarrow e^- + \nu_\mu + \bar{\nu}_e$) but have a lifetime of $\tau_\mu = 2.2\,\mu$s so they can be regarded as nearly stable when dealing with electromagnetic processes.

Experiments to measure the Lamb shift in muonic hydrogen have long been suggested as likely to lead to significant improvement in the determination of the proton radius, but that was no achieved until as recently as 2010 because of the considerable experimental challenges in dealing with this exotic atom.

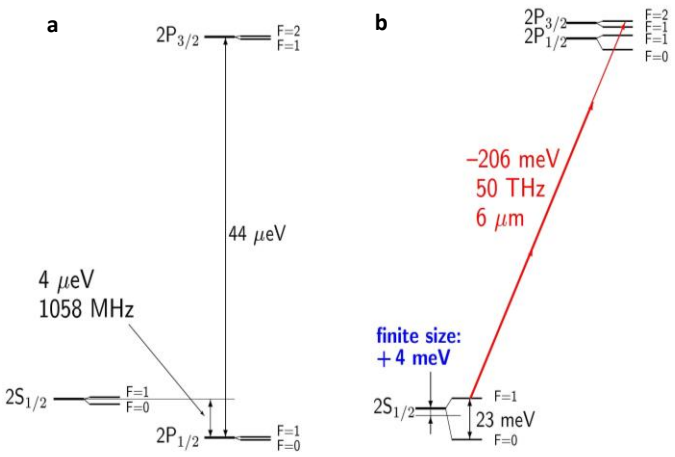

FIG. 3: **a.** Schematic layout, not to scale, of the 2S and 2P hydrogen energy levels; the Lamb shift is about 4 μeV. **b.** Schematic layout of the same energy levels for muonic hydrogen where the Lamb shift accounts for 206 meV. Note also the different relative position of the $2S_{1/2}$ and $2P_{1/2}$ in the two atoms. Figure taken from [10].

A. First measurement of the Lamb shift in muonic hydrogen (2010)

The goal of this experiment [5] performed at the Paul Scherrer Institute (Switzerland) is to measure the $2S-2P$ energy difference in μp atoms by laser spectroscopy and to deduce the charge radius of the proton with 10^{-3} precision, an order of magnitude better than ever previously measured.

The experiment is based on the measurement of the energy difference between the $2S_{1/2}^{F=1}$ and $2P_{3/2}^{F=2}$ muonic energy levels, see Fig. 4c. This transition was chosen because it gives the largest signal of all six allowed optical $2S-2P$ muonic transitions. In the setup of the experiment, negative muons from a low-energy muon beam are stopped in H_2 gas at 1 hPa, where highly excited μp atoms are formed. Practically all of them de-excite to the 1S ground state. However, there is about 1% probability for the long-lived 2S state to be populated. Using a laser pulse, transitions of the muons from the $2S$ state to the $2P$ state are induced on resonance at $\lambda \approx 6\,\mu$m, see Fig. 4a. Immediately, the $2P \rightarrow 1S$ deexcitation of the muon takes place by emitting a 1.9 keV X-ray (lifetime $\tau_{2P} = 8.5$ ps), see Fig. 4b. Detection in a narrow time window distinguishes the laser-induced X-rays from the background X-rays from other unwanted produced states and from muon decays. The lifetime of the μp $2S$ state is of importance in the experiment, because in absence of collisions, τ_{2S} would be equal to the muon lifetime of 2.2μs. But in the H_2 gas collisions between atoms may cause "prompt" deexcitations of the $2S$ state. The 1hPa pressure of the H_2 gas cavity is a trade-off between maximizing τ_{2S} (requiring low pressure) and minimizing the muon stop volume (requiring high pressure), which minimizes the laser pulse energy required to drive the wanted transition.

The relation between the measured energy of the $2S_{1/2}^{F=1} - 2P_{3/2}^{F=2}$ muonic transition and r_p requires detailed calculations of relativistic, QED and recoil corrections to the energies of the 2S and 2P states, some of which are proton charge-radius dependent, as well as the hyperfine splitting predictions.

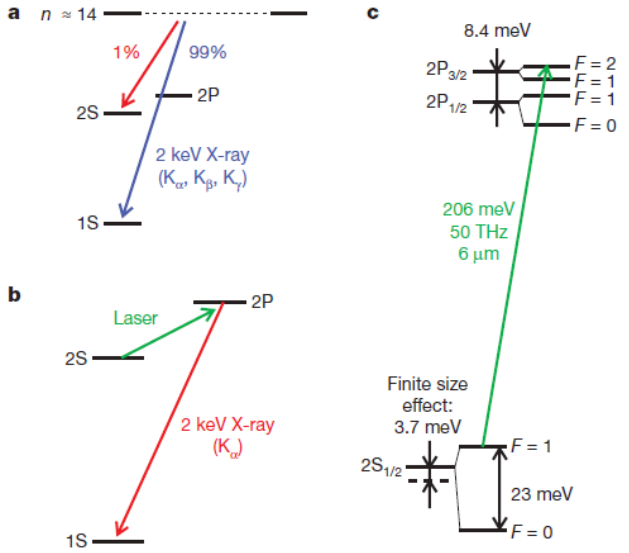

FIG. 4: **a.** Cascade deexcitation to the ground state as soon as the μp atom is formed. **b.** Laser pulse excitation to the 2P energy level and subsequent deexcitation to the 1S ground state. **c.** Lamb shift energy splitting, finite size effects and hyperfine structure. The green arrow represents the laser pulse excitation of the muon. Figure taken from [5].

These calculations have been performed in the literature and the corresponding results and references to the original authors can be found in [5] and in table 2.2 in [10]. From these contributions the total predicted $2S_{1/2}^{F=1} - 2P_{3/2}^{F=2}$ energy difference is obtained as

$$\Delta\tilde{E} = 209.9779(49) - 5.2262r_p^2 + 0.0347r_p^3 \text{ meV}, \quad (10)$$

where r_p is expressed in fm and numbers in parenthesis indicate the 1 standard deviation uncertainty of the last digits of the value.

The largest contribution in (10) comes from vacuum polarization effects and the second largest correction to the energy levels is given, in muonic hydrogen, by nuclear-size effects and accounts for about 2% of the $2S - 2P$ Lamb shift.

Vacuum polarization for muonic hydrogen. In μp atoms, where states are more sensitive to QED effects, vacuum polarization is the most important contribution to the Lamb shift (Fig. 3 shows how much more relevant the muonic Lamb shift is compared to ordinary hydrogen's Lamb shift).

The radius of the muonic atom becomes of the same order as the electron Compton wavelength λ_e, which approximately describes the size of the charge distribution of the e^+e^- pairs produced by the vacuum polarization. Therefore, the muon's wave functions of S-states overlap strongly with the charge distribution of the virtual e^+e^- pairs. This effect is treated with the Uehling potential [9] and gives in μp atoms a contribution to the Lamb shift of 205.0282 meV [10]. Other smaller contributions containing relativistic recoil, self-energy and higher-order corrections [12] have to be taken into account to finally obtain the first term in (10).

Nuclear size effects. The last two terms in (10) are the finite-size contributions to the 2S-2P energy splitting. Because the muon is much heavier than the electron its orbit around the proton is much smaller, making it more sensitive to the nuclear structure. The leading finite-size effect is given by eq. (7) where we see that the nuclear size effects scale with the reduced mass of the system and it gives a correction of $-5.1975r_p^2$. This represents a contribution of -3.98 meV, taking $r_p = 0.875$ fm, which is two orders of magnitude larger than for H. All main contributions related to the proton finite size are given in [5,10,11] and lead to the result quoted in eq. (10).

Fine and hyperfine structure. In order to determine the "pure" Lamb shift from the 2S-2P transition it is required to know fine and hyperfine contributions to the $n = 2$ state. The fine structure of the 2P states can be calculated for μp using the relativistic Dirac energies, taking into account recoil corrections and other effects [10]. The total result is:

$$\Delta E^{FS}\left(2P_{3/2} - 2P_{1/2}\right) = 8.352 \text{ meV}. \quad (X)$$

In hydrogen the hyperfine splitting has been measured with tremendous accuracy. Therefore, the Lamb shift in hydrogen can be extracted using the measured HFS value. For muonic hydrogen, however, there is not a measurement of the hyperfine splitting available up to date so theoretical predictions of the HFS of the muonic levels must be used. The hyperfine energy shifts are calculated including radiative, recoil and finite-size corrections. The result for the muonic hydrogen [12,13] is:

$$\Delta E^{HFS}\left(2P_{3/2}^{F=2}\right) = 1.2724 \text{ meV}, \quad (Y)$$
$$\Delta E^{HFS}\left(2S_{1/2}^{F=1}\right) = -5.7037 \text{ meV}.$$

The results (X) and (Y) add up to a total contribution to the $2S_{1/2}^{F=1} - 2P_{3/2}^{F=2}$ energy difference of $\Delta E^{F+HFS} = 3.9207$ meV.

In the experiment [5], it was obtained that the frequency of the laser to induce the $2S_{1/2}^{F=1} - 2P_{3/2}^{F=2}$ transition corresponds to an energy of $\Delta\tilde{E} = 206.2949(32)$ meV. From eq. (10), a proton charge radius of $r_p = 0.84184(36)(56)$ fm is deduced [5]; where the first uncertainty is experimental and the second one comes from the first term in (10). This new value of the proton radius is 10 times more precise than the previous world average mainly inferred from H spectroscopy but 5 standard deviations smaller.

We note that an additional term of +0.31meV in eq. (10) would be needed to match the measured $\Delta\tilde{E}$ energy difference with the CODATA value $r_p = 0.8768(69)$ fm.

B. Second experiment with muonic hydrogen (2013)

To further verify the previous result, a second experiment with muonic hydrogen was performed [6] in 2013. In order to rule out some possible error arising from theoretical predictions, two energy transitions were measured. In the new experiment, the muonic energy transition $2S_{1/2}^{F=0} - 2P_{3/2}^{F=1}$ was measured as well as the previously studied transition $2S_{1/2}^{F=1} - 2P_{3/2}^{F=2}$, see Fig. 5, using the same method of laser spectroscopy. The measurement of the two transitions allowed for an extraction of the proton radius r_p without relying on the theoretical predictions of the hyperfine splitting of the 2S muonic energy level, and only theoretical predictions of the HFS for the 2P energy levels were still needed.

The new value $r_p = 0.84087(39)$ fm obtained is 1.7 times more precise than the previous measurement of 2010 with muonic hydrogen and in agreement with it, but still in

strong disagreement with the CODATA value, therefore reinforcing the "proton radius puzzle".

Let us mention that, in 2016, the same team performed another laser spectroscopy experiment [14] in order to shed some light to the proton radius puzzle. This time the atom used was muonic deuterium, μd, composed of a nucleus with a proton and a neutron. Currently, nuclear masses of the proton and the neutron are accurately known, this allows one to appropriately link the atomic transition frequencies from H with the ones from deuterium. Therefore, it's possible to obtain the proton charge radius from the determination of the deuteron charge radius [14]. The new proton radius value extracted r_d gives a proton radius $r_p = 0.8356(20)$ fm, which is slightly below the muonic hydrogen measurements but still confirming the "shrinkage" of the proton radius.

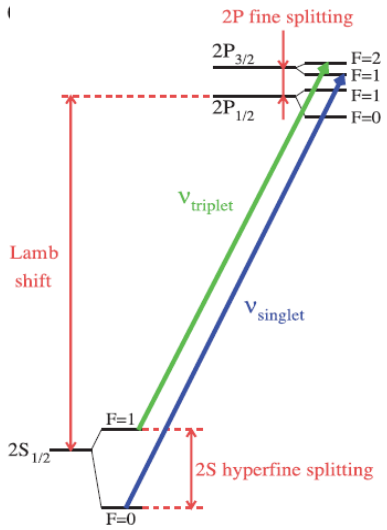

FIG. 5: 2S an 2P levels in mounic hydrogen and the measured transitions ν_s and ν_t. Figure taken from [6].

IV. RECENT EXPERIMENTS WITH HYDROGEN

When reviewing earlier experiments with precision laser spectroscopy in H, one notes [15] that the measurements were limited by the electron-impact excitation used to produce H atoms in an excited state, resulting in additional corrections to consider. In a new experiment [15] performed in 2017 with hydrogen, the experimental set up allowed the measurements to be essentially unaffected by these systematic effects. A new data analysis specially developed for this measurement was also used to treat the results. In the experiment, two transition frequencies were measured: the very well-known hydrogen transition 1S-2S and the 2S-4P transition. For brevity we will not further discuss the experiment here, details and specific calculations can be found in [15] and references quoted within. The results obtained are the most accurate from all H spectroscopy world data.

In this particular case, it was simultaneously determined r_p and R_∞ (we see in eq. (1) that atomic energy levels also depend on the Rydberg constant), giving a new value for the proton charge radius of 0.8335(95) fm, that is in good agreement with the μp value but still in disagreement with the CODATA value.

V. CONCLUSIONS

In this work, we have revised atomic energy levels for hydrogen-like atoms, focusing on muonic hydrogen, which we have seen is a good candidate to help us obtain a better measurement of the proton radius. We have given an overview of the different experiments performed on muonic hydrogen and its results in the calculations of the proton charge radius. The so-called "proton radius puzzle" has been intriguing scientists for a while and its origins are still far to be understood. Nonetheless, some possible explanations have been proposed. Assuming experimental results are correct one can ask whether the QED corrections are complete or maybe higher order contributions have been undervalued or even dismissed. The most recent discussion of these possible deficiencies can be found in [12]. Another suggestion has been assuming a further particle-antiparticle fluctuation beyond e^+e^- and $\mu^+\mu^-$ but it is still left to investigate the influence of such effects on energy levels of muonic hydrogen. On the other hand, provided that QED calculations are correct, new experiments with improved accuracy can provide additional experimental data and help understand the discrepancy.

One thing is clear, even with the proton being the single most common particle around us, some of its properties are still not well understood. The proton radius puzzle has questioned the correctness of various experiments and quantum electrodynamics calculations, the value of the Rydberg constant, our understanding of the proton structure and the standard model of particle physics.

Acknowledgments

I would like to thank my advisor Mario Centelles, for his help with this work, and my family for helping me through all these years.

[1] I. Sick, *Phys. Lett. B* **576**, 62 (2003).
[2] P.G. Blunden and I. Sick, *Phys. Rev. C* **72**, 057601 (2005).
[3] M. Niering et al., *Phys. Rev. Lett.* **84**, 5496 (2000).
[4] C. Schowb et al., *Phys. Rev. Lett.* **82**, 4960 (1999).
[5] R. Pohl et al., *Nature* **466**, 213 (2010).
[6] A. Antognini et al., *Science* **339**, 417 (2013).
[7] M.I. Eides et al., *Physics Reports* **342**, 63-261 (2001).
[8] W.E. Lamb and R.C. Retherford, *Phys. Rev.* **72,** 241 (1947).
[9] W. Greiner and J. Reinhart, "Quantum electrodynamics", 3rd ed (Springer, Berlin, 2003).
[10] A. Antognini, "The Lamb shift experiment in muonic hydrogen", PhD Thesis (2005). *https://edoc.ub.uni-muenchen.de/5044/*
[11] J.L. Friar, *Ann. Phys (NY)* **122**, 151 (1979).
[12] E.Borie, *Phys. Rev.* A **71,** 032508 (2005).
[13] A.P. Martynenko, *Phys. Rev*. A **71,** 022506 (2005).
[14] A. Beyer et al., *Science* **358**, 79 (2017).
[15] R. Pohl et al., *Science* **353**, 669 (2016).